European Journal of
Immunology

HIGHLIGHTS

Clinical

FRONTLINE | Research Article

Expansion of plasmablasts and loss of memory B cells in peripheral blood from COVID-19 patients with pneumonia

Sara De Biasi[*1], *Domenico Lo Tartaro*[*1], *Marianna Meschiari*[2], *Lara Gibellini*[1], *Caterina Bellinazzi*[1], *Rebecca Borella*[1], *Lucia Fidanza*[1], *Marco Mattioli*[1], *Annamaria Paolini*[1], *Licia Gozzi*[1], *Dina Jaacoub*[2], *Matteo Faltoni*[2], *Sara Volpi*[2], *Jovana Milić*[2], *Marco Sita*[3], *Mario Sarti*[4], *Carlo Pucillo*[5] (iD), *Massimo Girardis*[3], *Giovanni Guaraldi*[2], *Cristina Mussini*[2] and *Andrea Cossarizza*[*1,6] (iD)*

[1] Department of Medical and Surgical Sciences for Children and Adults, University of Modena and Reggio Emilia School of Medicine, Modena, Italy
[2] Infectious Diseases Clinics, AOU Policlinico and University of Modena and Reggio Emilia, Modena, Italy
[3] Department of Anesthesia and Intensive Care, AOU Policlinico and University of Modena and Reggio Emilia, Modena, Italy
[4] Clinical Microbiology Unit, AOU Policlinico, Modena, Italy
[5] Laboratory of Immunology, Department of Medicine, University of Udine, Udine, Italy
[6] National Institute for Cardiovascular Research, Bologna, Italy

Studies on the interactions between SARS-CoV-2 and humoral immunity are fundamental to elaborate effective therapies including vaccines. We used polychromatic flow cytometry, coupled with unsupervised data analysis and principal component analysis (PCA), to interrogate B cells in untreated patients with COVID-19 pneumonia. COVID-19 patients displayed normal plasma levels of the main immunoglobulin classes, of antibodies against common antigens or against antigens present in common vaccines. However, we found a decreased number of total and naïve B cells, along with decreased percentages and numbers of memory switched and unswitched B cells. On the contrary, IgM$^+$ and IgM$^-$ plasmablasts were significantly increased. In vitro cell activation revealed that B lymphocytes showed a normal proliferation index and number of dividing cells per cycle. PCA indicated that B-cell number, naive and memory B cells but not plasmablasts clustered with patients who were discharged, while plasma IgM level, C-reactive protein, D-dimer, and SOFA score with those who died. In patients with pneumonia, the derangement of the B-cell compartment could be one of the causes of the immunological failure to control SARS-Cov2, have a relevant influence on several pathways, organs and systems, and must be considered to develop vaccine strategies.

🖥 Additional supporting information may be found online in the Supporting Information section at the end of the article.

Correspondence: Andrea Cossarizza
e-mail: andrea.cossarizza@unimore.it

*De Biasi, Tartaro, and Cossarizza contributed equally to the study.
[Correction added on 17 August 2020, after first online publication: URL for peer review history has been corrected.]

Introduction

COronaVIrus Disease 19 (COVID-19) is caused by a coronavirus, called severe acute respiratory syndrome coronavirus-2 (SARS-CoV-2), that has been detected in humans at the end of 2019 and has provoked the pandemic that we all are experiencing. Most infections are asymptomatic, but some individuals can present with a wide spectrum of clinical manifestations, ranging from viral pneumonia to respiratory failure, or can develop an acute respiratory distress syndrome (ARDS), with reported mortality rates ranging from 20-90% [1,2]. Different therapies are now demonstrating benefit, and biological drugs, such as tocilizumab, that can block the activity of IL-6 seem effective at reducing mortality [3].

Understanding the pathophysiology of the immune response to this virus is fundamental to develop targeted therapies and vaccines aimed to control and eradicate the virus [4]. The virus mainly infects airways and alveolar epithelial cells, and can interact with cells coexpressing the surface receptors angiotensin-converting enzyme 2 (ACE2) [5] and the type II transmembrane serine protease TMPRSS2 [6]. The internalization exposes the genomic RNA to the dsRNA sensing machinery in the cell IRF-3 cascade leading to the induction of *IFNb* and the production of secreted IFN-β protein by DCs [7] while the expression of viroporin 3a triggers the activation of NOD-like receptor protein 3 (NLRP3) inflammasome and the secretion of IL-1β in BM-derived macrophages, suggesting the induction of cell pyroptosis [8]. Macrophages recognition of released damage-associated molecular patterns (DAMPs) or pathogen-associated molecular patterns (PAMPs) induces a strong secretion of pro-inflammatory cytokines and chemokines, such as IL-1β, IFN-γ, M1p-2, among others, that shape the immune response [9] and polarize T cell toward Th1 response [10]. In turn, these cells are crucial to prime $CD8^+$ T cells and to help the differentiation of B cells into antibody-secreting cells and plasma cells.

In SARS-CoV, a B-cell response arises about 7-10 days after onset of symptoms, and in 3 weeks some, but not all, patients can develop neutralizing antibodies [11], first against the viral N protein, and then for the S protein. However, significant individual differences exist, since a relevant subset of patients do not develop a long-lasting immune response to SARS-CoV-2, suggesting that they could undergo reinfection [12]. Moreover, the almost simultaneous expression of IgM and IgG present in several cases suggests that the humoral immune response has remarkable peculiarities both in the activation of memory and naïve B-cell subpopulations.

Herein, we asked whether B cells from COVID-19 patients showed alterations linked to cell exhaustion or activation. We found a significant increase in plasmablasts, expressing or not IgM, with a decrease in switched and unswitched memory B cells. This result is indicative of a rapid expansion of B cells subset triggered by the cytokine storm, particularly IL-6. Interestingly, in vitro stimulation of T lymphocytes by specific stimuli resulted in a secondary, almost nonspecific expansion of B cells.

Results

COVID-19 patients show a normal pattern of plasma antibodies

Patients had normal amounts of different classes of Ig, along with normal amounts of the antibodies that are induced by the common pathogens or by different vaccines, as described above (Table 1). At blood collection, in all patients but two we could detect antibodies against the virus. However, one patient had IgG only, and in two patients IgG plasma levels were relatively higher than IgM^+ IgA.

COVID-19 patients show changes in the percentage and absolute number of B cells

To finely characterize peripheral B cells in subjects affected by COVID-19 pneumonia, we studied patients and controls using polychromatic flow cytometry. The analysis of the data resulting from cytofluorimetric analysis was then performed by using two complementary methodologies. In the first, we used the classical approach based upon the two-dimensional recognition of a given cell type (for example, cells expressing two markers), followed by a first gate that was required to identify the population of interest, followed by sequential gates to identify other markers such as those of activation or differentiation. Data obtained with this gating strategy were then analyzed by appropriate, nonparametric statistical tests, and represented in the figures as scatter plots with means and standard errors of the mean. In the second, we performed an unsupervised analysis that considers the entire, complex scenario presented by B cells. This analytical technique uses the multidimensional information obtained by Flow-SOM metaclustering coupled to a dimension-reduction method such as the Uniform Manifold Approximation and Projection (UMAP). Heat maps finally report statistical analysis (see Methods for details).

The gating strategy for the identification of different types of B cells, performed by previously described classical methods [13], is shown in Fig. 1. Panel A shows that after a preliminary gate on the parameters "time" and "viability," we could identify lymphocytes on the basis of side scatter and CD45 expression, then we could exclude aggregates, gate on single cells, and analyze CD19+ B cells. Among them, we identified those that expressed IgM or IgD, or both, or that were double negative. Panel B, related to cells that were negative for both IgD and IgM, shows representative examples of the populations present among $CD21^+$, $CD24^+$ or $CD21^-$, $CD24^-$ cells. Note that a control donor and a COVID patient had different percentages of memory switched of plasmablasts. Figure 1C, related to cells that were IgD^- and IgM^+, shows that also the amount of IgM^+ plasmablasts (expressing CD27 and CD38) was different between a patient and a control donor.

The same Fig. 1 indicates the percentages and absolute numbers of different B-cell populations. Patients and controls

Table 1. Anti-SARS-CoV-2 and plasma levels of different antibodies in patients with Covid-19 pneumonia

Patient ID	1	2	3	4	5	6	7	8	9	10	11	Reference Values
Anti-SARS-CoV2 IgG	1.5	3.0	25.9	1.5	2.3	16.5	6.6	2.5	20.7	1.6	12.1	<4 negative; >6 positive
Anti-SARS-CoV2 IgM+ IgA	5.5	38.6	38.2	23.2	13.3	32.5	34.4	4.0	40.6	8.3	5.5	<6 negative; >8 positive
Total IgG	731	1626	1338	914	924	710	808	849	784	739	876	700- 1600 mg/dL
Total IgA	301	141	208	340	254	252	167	460	164	147	131	70-400 mg/dL
Total IgM	43	85	74	131	97	155	81	195	76	187	36	40- 230 mg/dL
Rubella IgG EIA	291	291	291	4	254	47	4	20	76	16	53	>6 positive
Rubella IgM EIA	0.02	0.03	0.01	0.49	0.03	0.03	0.01	0.02	0.01	0.02	0.03	<0.10 negative
Herpes Simplex Virus 1 IgG CLIA	99	203	2	88	2	148	200	112	48	237	126	<negative
Herpes Simplex Virus 2 IgG CLIA	33	1	1	1	157	1	1	1	3	1	3	<10 negative
Herpes Simplex Virus 1/2 IgM CLIA	9	1	1	1	1	1	2	4	1	2	1	<20 negative
Varicella Zoster IgG EIA	1050	783	720	2,850	1,320	1,040	884	259	689	274	1620	<50 negative
Varicella Zoster IgM EIA	0.03	0.01	0.02	0.06	0.05	0.03	0.01	0.01	0.01	0.02	0.01	<0.10 negative
Measle IgG EIA	3630	19 300	19 100	17 700	10 700	1020	3420	17 000	923	1990	16 700	<150 negative
Measle IgM EIA	0.01	0.01	0.01	0.04	0.02	0.01	0.02	0.09	0.01	0.04	0.02	<0.10 negative
Parotitis IgG EIA	0.3	2.58	0.68	0.15	1.06	0.64	1.26	0.36	0.32	0.22	0.79	<0.10 negative
Parotitis IgM EIA	0.05	0.11	0.02	0.13	0.03	0.01	0.28	0.05	0.01	0.03	0.07	<0.10 negative
Influenza A IgG EIA	5.8	13.3	25.1	23.2	15.7	12.9	17.2	11.7	35.1	9.6	34.5	<8.5 negative
Influenza A IgA EIA	2.8	1.8	3.7	6.7	2.8	4.4	2.2	4.6	8.8	3.4	17.3	<8.5 negative
Influenza B IgA EIA	3.3	1.9	2.5	4.5	3.3	1.6	2.4	7.1	3.2	2.4	3.1	<8.5 negative
Influenza B IgG EIA	9.2	9.3	26.1	19.6	9.4	8.1	16.3	10.3	12.5	13.6	19.1	<8.5 negative
Bordetella pertussis IgG EIA	6	2	12	3	22	7	1	1	1	25	2	<40 no recent infection
Bordetella pertussis IgA EIA	5	3	5	3	9	8	4	10	1	1	2	>12 recent infection
Tetanus toxoid IgG EIA	0.03	0.01	1.05	1.12	0.09	0.96	1.69	0.06	0.54	0.25	2.29	<0.10 not protected

had a similar percentages of total or naïve B cells, but in patients the absolute number was statistically lower (panel D). An increased percentage, but not number, of transitional B cells was also found. Patients had lower percentages and absolute numbers of memory switched and memory unswitched B cells, but similar amounts of memory IgM-only cells (panel E). Panel F shows that the percentages and absolute numbers of IgM− plasmablasts, IgM+ plasmablasts, and of total plasmablasts were significantly higher in patients when compared to controls.

Fine detection of B-cell alterations in COVID-19 patients

We used a more sophisticated approach to detect fine changes occurring within different subpopulations of CD19+ B cells. For each patient and control, data from 5000 B lymphocytes were exported and concatenated in a unique matrix. We explored the B-cell panel by unsupervised analysis using FlowSOM [14]; this performs multivariate clustering of cells based on the self-organized map (defined "SOM") algorithm, categorizing cells into relevant
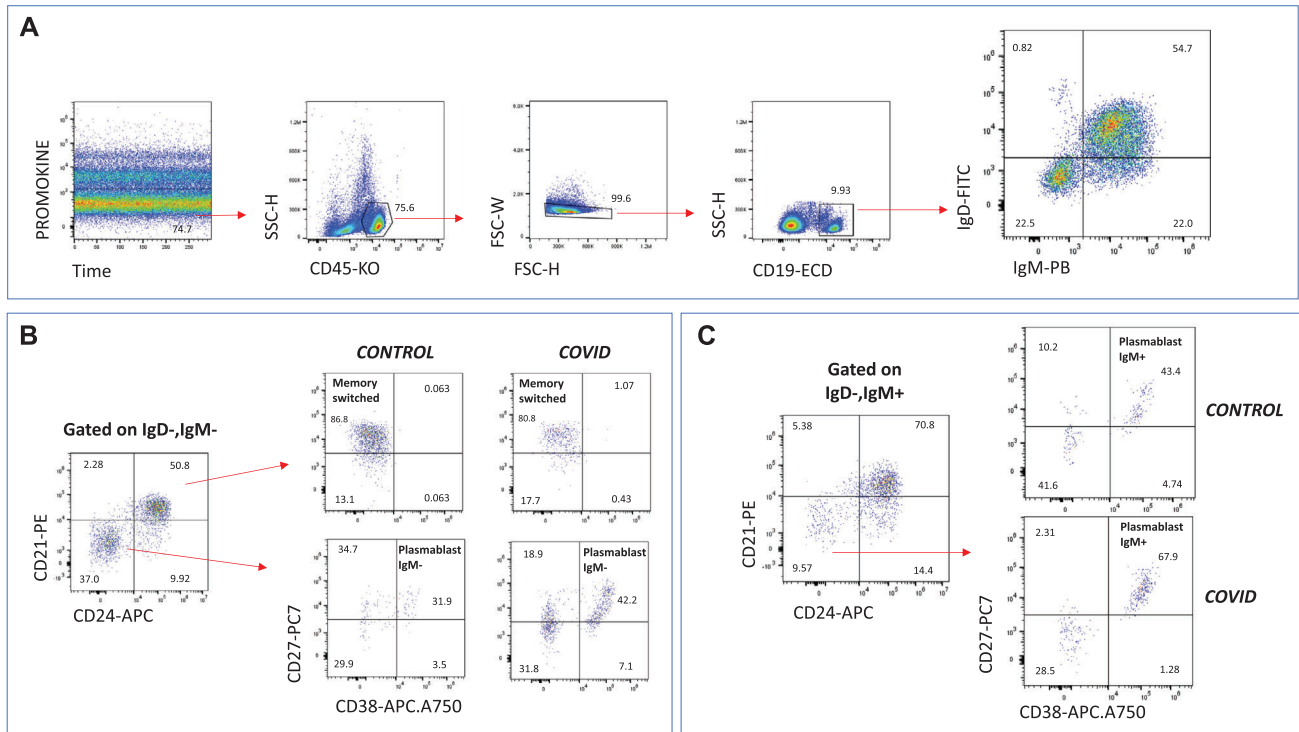
Figure 1. Identification of different B-cell populations. (A) Gating strategy used to identify B cells expressing IgM or IgD on their plasma membrane. A first gate was set in living cells and time, then on CD45$^+$ cells, on physical parameters (FSC-H vs FSC-W) to eliminate doublets, then on CD19 that identify B cells. (B) Representative example of the analysis of the expression of CD27 and CD38 on different types of CD19+, IgM$^-$, IgD$^-$ lymphocytes that were double positive or double negative for CD21 and CD24. This analysis was performed to identify memory switched and IgM$^-$ plasmablasts. A COVID patient and a control donor are shown. (C) Representative example of the analysis of the expression of CD27 and CD38 on different types of CD19$^+$, IgM$^+$, IgD$^-$ lymphocytes. This analysis allowes to identify IgM$^+$ plasmablasts. A COVID patient and a control donor are shown. (D) Percentage and absolute number of CD19$^+$ B cells, naïve B cells, and transitional B cells in COVID patients (red) and healthy donors (black). (E) Percentage and absolute number of memory switched, memory IgM$^+$ only and memory unswitched B cells in COVID patients (red) and healthy donors (black). (F) Percentage and absolute number of IgM$^-$, IgM$^+$, and total plasmablasts in COVID patients (red) and healthy donors (black). Data in A-C are from a single experiment representative of 25 phenotypic analysis performed in 14 COVID patients and 11 healthy donors. Data in E-F are shown as single values (dots), with lines that indicate the mean ± SEM, and represent all the aforementioned analyses in 11 healthy controls (black) and 14 COVID patients (red). Mann–Whitney *t*-test was used; exact *p* value is reported in the figure, when significant.

metaclusters based on their surface markers. We first clustered all individual cells into nine distinct clusters based on the surface expression marker proteins. Naïve B cells are defined as IgM$^+$, IgD$^+$, CD24$^+$, CD21$^+$, CD38$^-$, CD27$^-$ while transitional B cells are IgM$^+$, IgD$^+$, CD24$^+$, CD21$^+$, CD38$^+$, CD27$^-$. Memory unswitched B cells are defined as IgM$^+$, IgD$^+$, CD24$^+$, CD21$^+$, CD38$^-$, CD27$^+$ while memory switched B cells are IgM$^-$, IgD$^-$, CD24$^+$, CD21$^+$, CD38$^-$, CD27$^+$. Memory IgM only B cells are IgM$^+$, IgD$^-$, CD24$^+$, CD21$^+$, CD38$^-$, CD27$^+$. Plasmablasts are IgM$^{-/+}$, IgD$^-$, CD24$^-$, CD21$^-$, CD38$^+$, CD27$^+$. Finally, we were able to identify a population of B cells called "unswitched CD24$^+$," which resemble a population of exhausted B cells as they are CD21$^-$ (Fig. 2A, left panel).

After this, we used a dimensionality reduction method, the UMAP to distinguish different CD19+ B-cell populations (Fig. 2A, right panel). It is possible to immediately recognize naïve B cells (red dots), memory unswitched (blue), memory switched (pink), as well as IgM$^-$ plasmablasts. The number of IgM$^+$ plasmablasts, even if evident in the left part of the left panel (in orange) was too low to allow any unsupervised analysis.

As shown in the heat map of Fig. 2B, naïve cells were similar among patients and controls. On the contrary, significant differences were present as far as almost all the other B-cell populations were concerned.

B-cell proliferation was similar in patients and controls

We could evaluate B-cell proliferation in seven patients and eight controls (Fig. 3). B cell were indirectly stimulated by the activation of T cells, that can to produce, among others, cytokines like IL-2 and IL-6, that in turn induce in vitro B-cell proliferation. Panel A shows the gating strategy used for this analysis. After a gate on cell dimension, we draw a gate to identify single cells and exclude doublets, then a gate to exclude dead cells, and a final gate to identify CD19+ B lymphocytes. Using CSFE allowed us to investigate either the proliferation index (i.e. the number of cells that were able to enter into the cell cycle) or the percentage of dividing cells (i.e. proliferating cells were
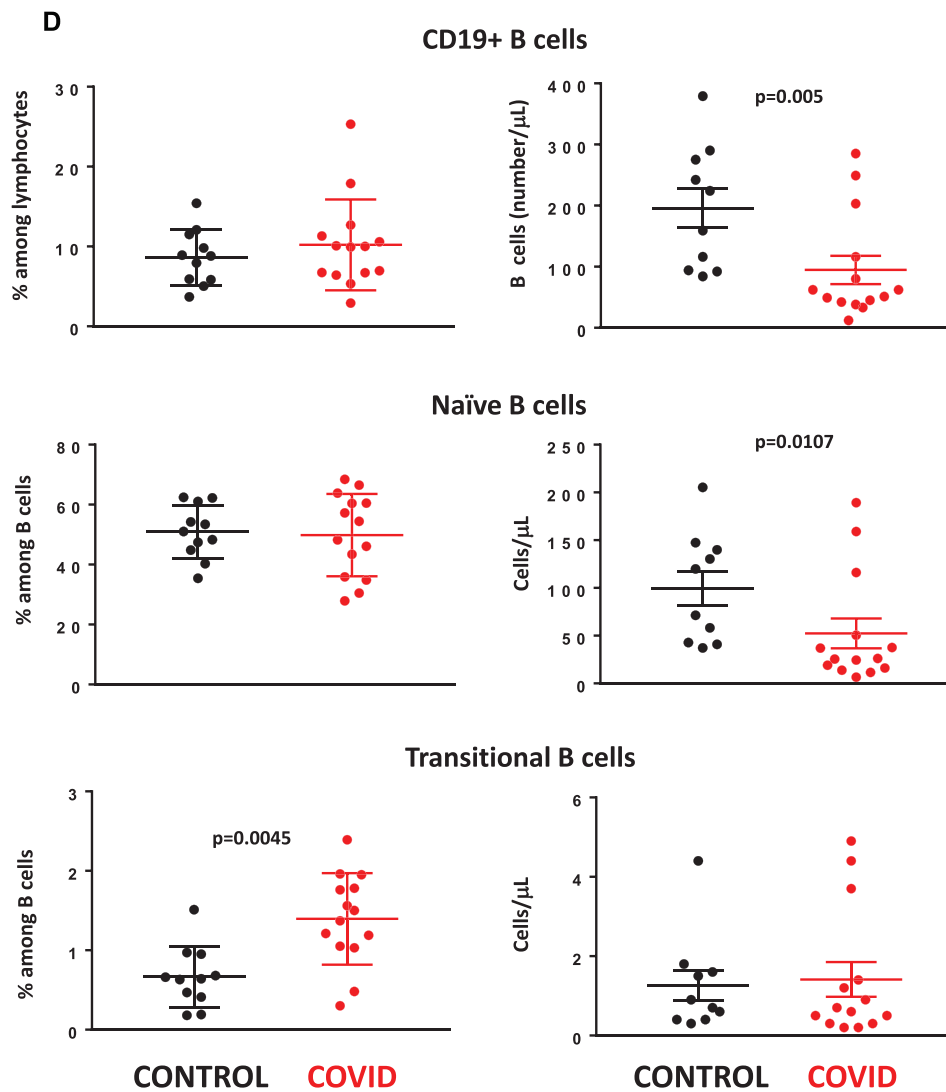
D

CD19+ B cells

Naïve B cells

Transitional B cells

Figure 1. *Continued.*

able to enter into more rounds of proliferation) (panel B). As shown in panel C, no differences were found between patients and controls.

PCA allows the identification of critical biomarkers associated with clinical outcome

Figure 4 shows that parameters, such as the absolute number of lymphocytes, platelets, total number of B lymphocytes, different types of B cells (memory switched and unswitched, memory IgM-only, transitional, naive), along with pO_2/FiO_2 and sO_2 clustered with the PCA area of patients who were discharged. On the contrary, IgM level, along with well expected clinical and biochemical parameters, such as SOFA score, heart rate, blood pH, CK, CRP, D-dimer, among others, clustered in the area of patients who died.

Discussion

To profile the SARS-CoV-2 humoral immune responses, we have investigated the B-cells compartment of COVID-19 patients with pneumonia admitted to Infectious Diseases Clinics (Modena, Northern Italy) in March-April 2020. All patients were lymphopenic, but most did not require invasive ventilation and did not suffer from too advanced disease. Three of them, however, died between 13 and 29 days after admission; in all patients, the analyses here reported were performed 2-4 days after admission. We found significant and global alterations in the B-cell compartment that underline the immune system's effort to make up for lymphopenia with the increase in transitional B cells and plasmablasts, besides the cytokine storm and the functional and phenotypic alterations of the T-cell compartment that we have recently described in this group of patients [14]. Of note, memory B cells, that are supposed to remain stable or slightly increase
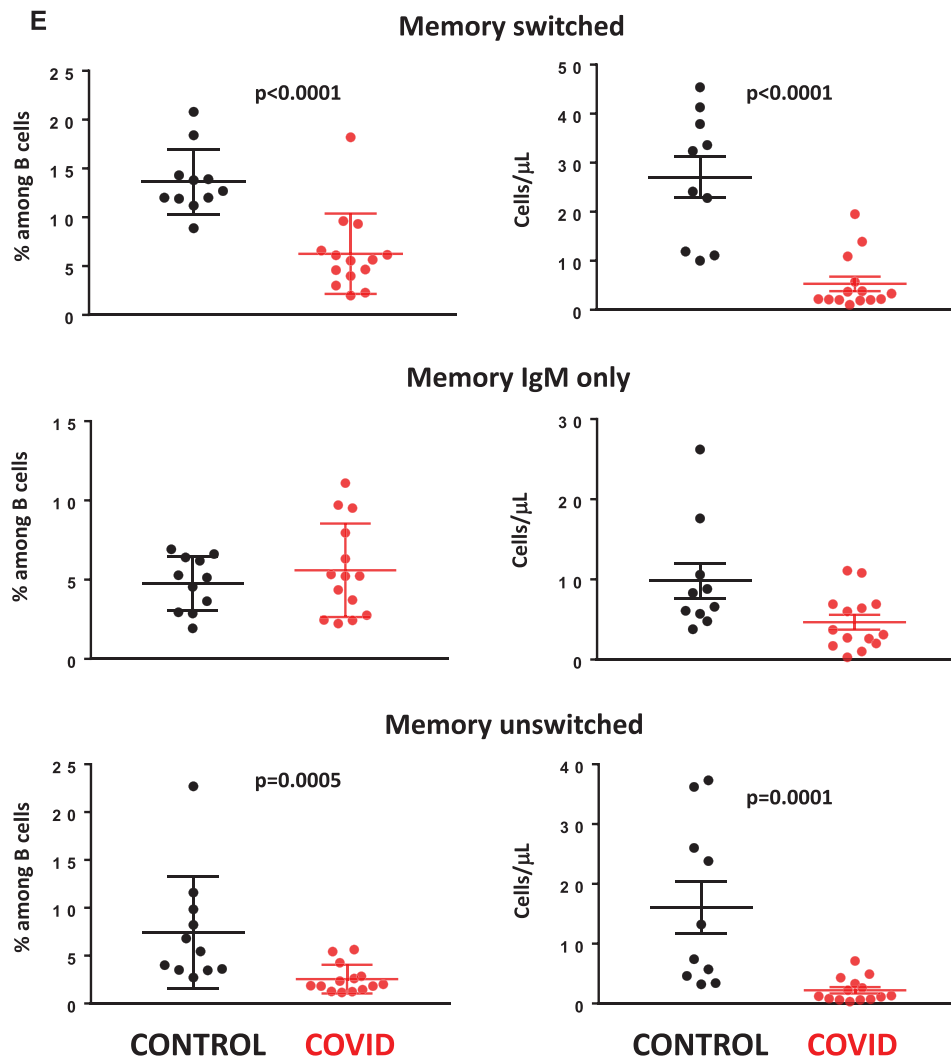
Figure 1. *Continued.*

from 20 to 80 years [15,16], in our patients were significantly lower than those of controls, who were younger. This further evidences how deep was the B-cell impairment that we have found.

Based on previous studies, immediate, primary inflammatory responses occurs early after a viral infection, and is mainly driven by an active viral replication. During coronavirus infection, the host response is associated with a viral-mediated downregulation and shedding of the virus-specific ACE-2 receptor [17]. Several molecular mechanisms are implicated in virus spreading, and obviously in the last months the peculiarity of the immune response to SARS-CoV-2 has been under deep investigation all over the world. However, little consideration has been dedicated to B cells and their capacity to secrete antibodies.

TNF-α and IL-6 are among the most represented cytokines in plasma from COVID-19 patients [14]. Both are involved in epithelial damage and lung fibrosis, but can also modulate B-cell differentiation, lifespan, and activation. IL-6 and TNF-α cooperate at different levels in the regulation of B-cell life and activity, acting

sequentially in the B-cells immune response [18-24]. Recently, we have described the characteristics of cytokine storm in a group of 39 patients with COVID-19 pneumonia that included also those here described [14]. In these patients, extremely high plasma levels of TNF and IL-6 were detected, but, likely because of the relatively low number of patients studied, we found no significant correlations between the number or the percentage of different B-cell populations and plasma levels of these cytokines (data not shown).

Likely, the presence of IgM and IgG observed in COVID-19 patients could be the result of antibodies produced by plasmablasts, which, to some extent, can be induced by a T-cell-independent Ig switch, typically limited to IgG3. Since no assays are currently available to investigate specific IgG subclasses, further studies are needed to confirm this aspect and clarify its importance. The increased presence of plasmablasts in patients suggests the involvement of innate B cells in the production of antibodies, along with the findings that in a few cases IgG, but not IgM were present in the plasma of recently infected patients.
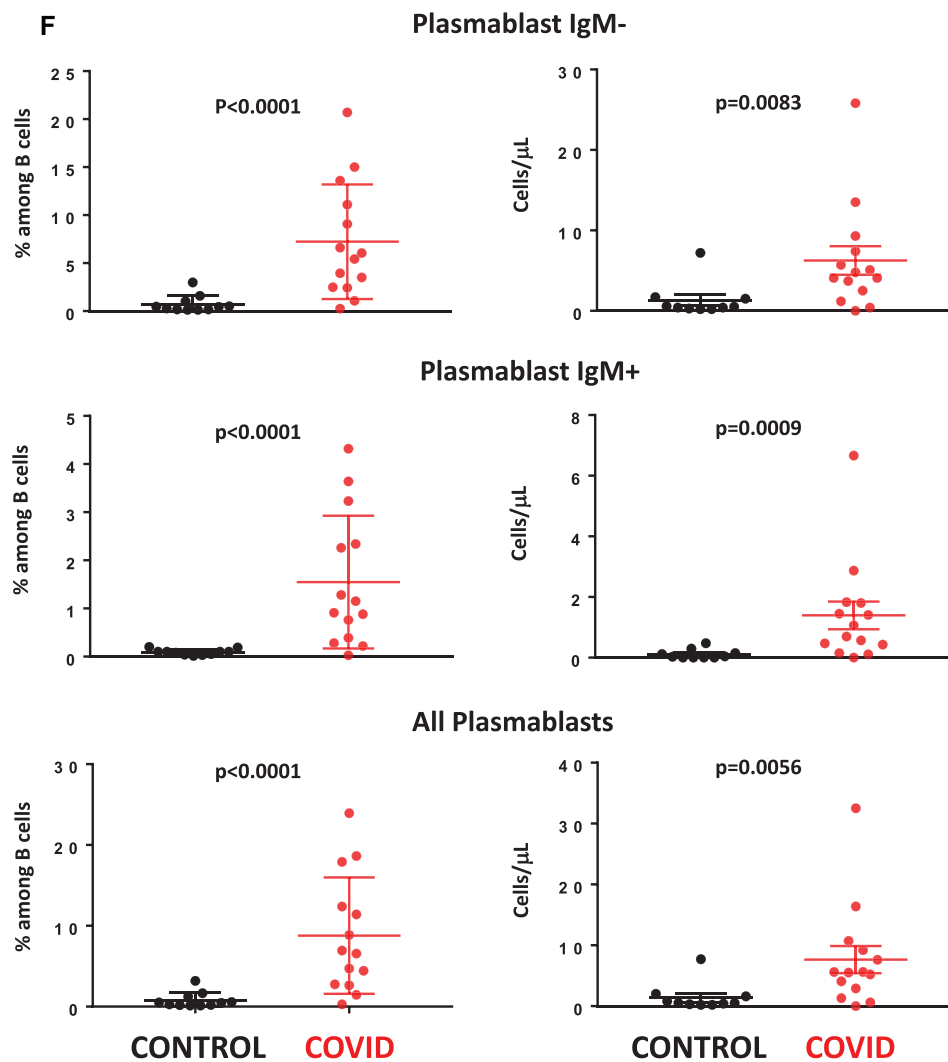
Figure 1. *Continued.*

This phenomenon advocates the expansion and secretion of immunoglobulins by pre-existing memory B-cells specific for a coronavirus different from SARS-CoV-2. Further studies are needed to better clarify this aspect.

We noted an increase in the percentage, but not in the absolute number of transitional cells (CD24++, CD38++), relatively immature elements that are migrating from the BM to peripheral lymphatic organs, where they develop into mature-naïve B cells (CD24+, CD38+). It remains to be established whether the relative expansion of these immature cells, along with that of IgM+ plasmablasts plays a role in generating or not an effective anti-SARS-CoV2 immune response.

We are well aware that our study has some limitations. First, we could investigate B-cell phenotype in a relatively low number of patients. Second, the age of controls was lower, but it has to be underlined that: (i) in the lockdown period, aged persons could not leave home, could not donate blood, and we had to study those volunteers who were available in our hospital; (ii) it

was not allowed, nor safe to go and collect blood in protected structures for aged individuals; (iii) even if the age of patients was higher than that of controls, the level of their memory B cells was significantly lower, although we would have expected otherwise. Third, we could perform functional analyses only in a few patients, who however showed the same proliferative capacity of controls. Fourth, due to the low number of patients, we could not find significant correlations between B-cell parameters and clinical outcome. However, the PCA-based approach showing the coclustering of B-cell populations, biochemical parameters, and crucial clinical endpoints (such as survival or death) further underlines the importance of the B-cell compartment, especially as far as memory cells are concerned.

In conclusion, our study provides novel contributions to the understanding of the breadth and kinetics of B-cell responses in COVID-19 patients. We show that the recruitment of partially mature B cells could indicate their exhaustion, as a resulting from the exaggerated immune activation that we have already
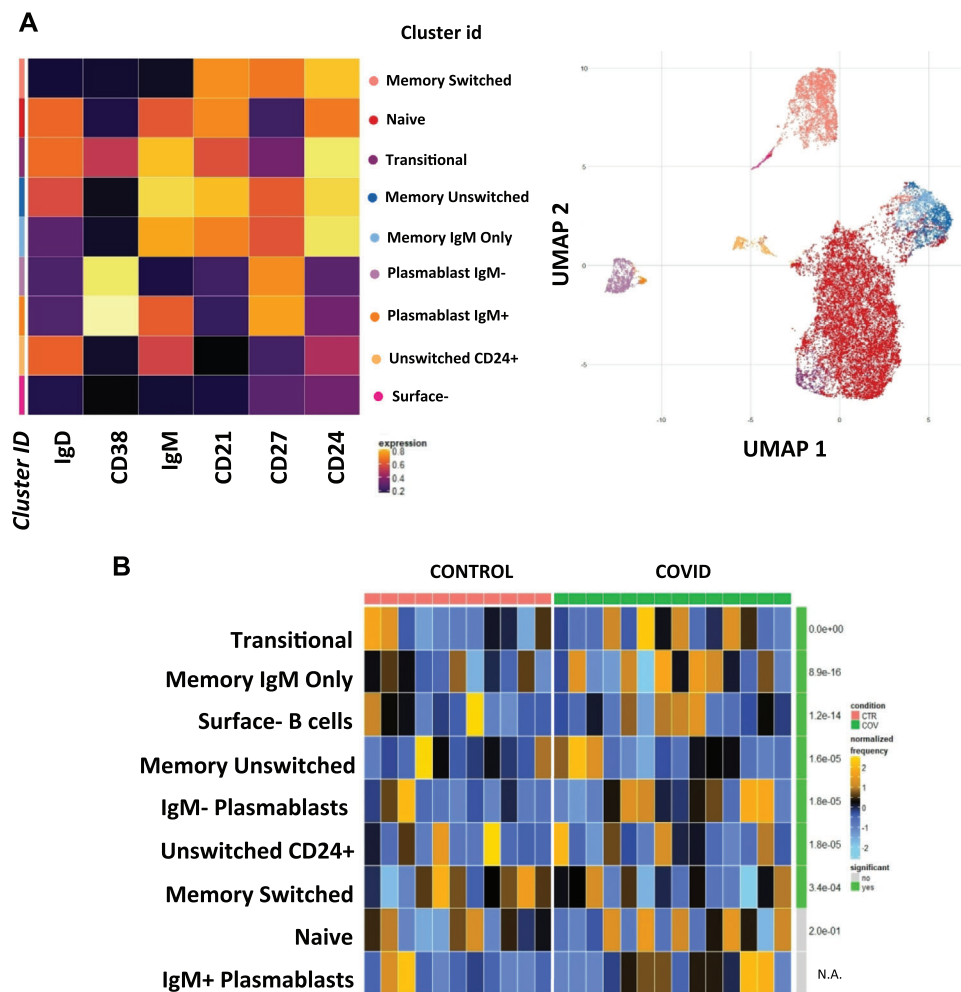
Figure 2. Unsupervised analysis of the B-cell compartment reveals profound alterations in COVID patients. (A) Left: heatmap representing different B-cell clusters identified by FlowSOM, with relative identity and percentages in all healthy controls and COVID-19 patients. The colors in the heatmap represent the median of the arcsinh, 0-1 transformed marker expression calculated over cells from all the samples, varying from black for lower expression to yellow for higher expression. Each cluster has a unique color assigned (bar on the left). CONTROL=11 donors, COVID=14. (A) Right: Uniform Manifold Approximation and Projection (UMAP) representation of the B-cell landscape. Each color is assigned according to the cluster identification palette. (B) Differential analysis between control (color:salmon) and COVID-19 patients (green). The heatmap represents arcsine-square-root transformed cell frequencies that were subsequently normalized per cluster (rows) to mean of zero and standard deviation of one. The color of the heatmap varies from pale blue indicating relative under-representation to yellow, indicating relative over-representation. Bar and numbers at the right indicate significant differentially abundant clusters (green) and adjusted *p*-values. Clusters are sorted according to adjusted *p*-values, so that the cluster at the top shows the most significant abundance changes between the two conditions. Due to the low number of cells, the analysis of IgM$^+$ plasmablasts was not possible (lower line, N.A.: not available). DiffCyt package was used to perform statistical analyses. This analysis has been performed on the raw and ungated data regarding the identification of B cells in 25 blood samples, obtained from 14 COVID patients and 11 healthy donors.

described [14]. We also propose that B cells, especially plasmablast, should be considered in the clinical evaluation and stratification of COVID-19 patients with different disease severity. Our data could be useful to design personalized therapeutical approaches or new interventions, or help in designing a vaccine. In this case, vaccination strategies should take into account not only the need to induce the production of neutralizing antibodies against the virus, but also the development of a long-standing, effective immunological memory and, possibly, the smoothing of inflammatory phenomena that can play on the side of the virus.

Materials and Methods

Study design

This is a case-control, cross-sectional, single-center study, approved by the local Ethical Committee (Area Vasta Emilia Romagna, protocol number 177/2020, March 10, 2020). Each participant provided informed consent and all clinical investigation have been conducted according to the Declaration of Helsinki principles. A total of 14 COVID-19 patients with pneumonia were
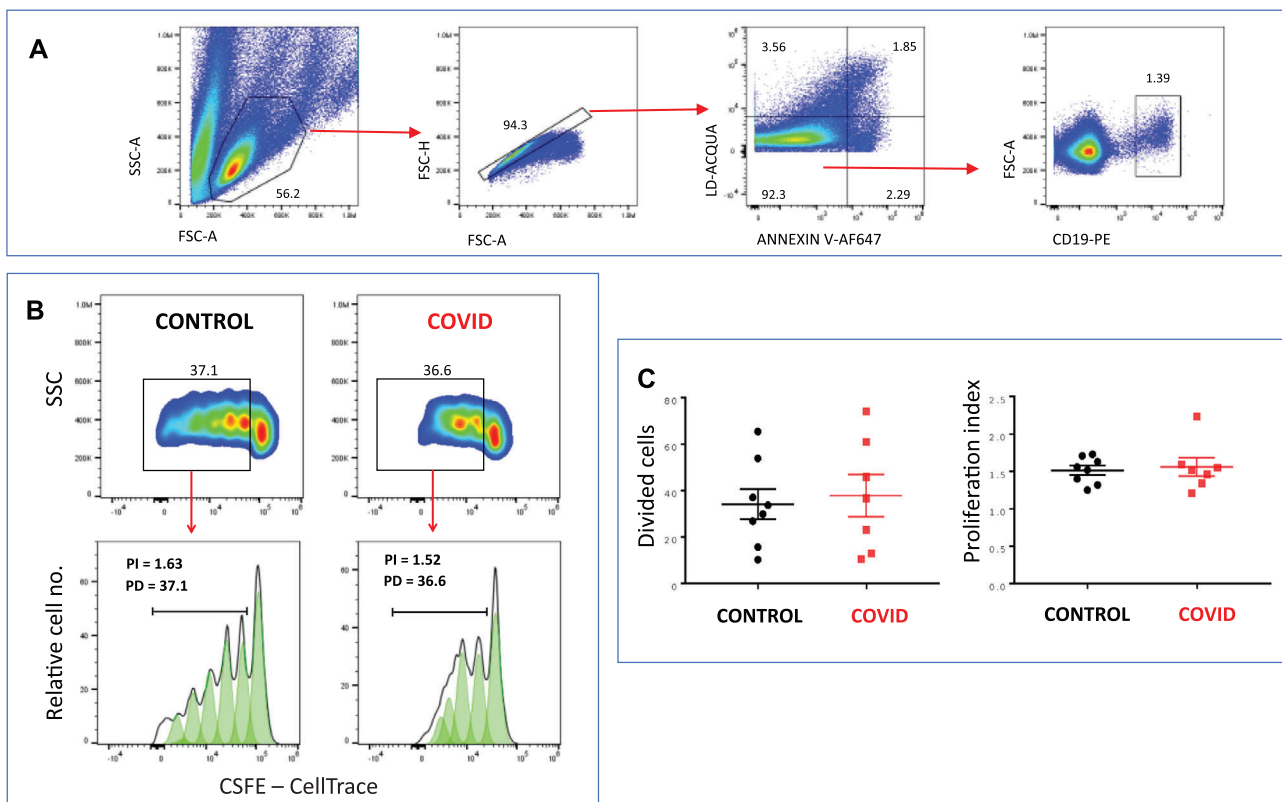
Figure 3. B-cell proliferation was similar in healthy controls and COVID patients. (A) Representative example (out of 15 experiments) showing the gating strategy used to identify B cells after 6 days of PBMC colture in the presence of anti-CD3 plus anti-CD28 mAbs and IL-2. A first gate was set on physical parameters, then on FCS-A abd FSC-W to eliminate doublets, that on live-death plus annexin V to eliminate dead cells, then on CD19+ events. These cells were then analyzed in panel B. (B) Representative example of the analysis of in vitro B-cell proliferation by the method of CSFE that allows the identification of dividing cells and proliferation index. The gates depicted in the upper panels and the bar in the lower panels identify proliferating cells. (C) Control donors (black dots) and COVID patients (red) showed similar amounts of B cells able to proliferate after in vitro stimulation. Mann–Whitney t-test was used; exact p value is reported in the figure, when significant. Data in C are shown as single values (dots), with lines that indicate the mean ± SEM, and represent all the aforementioned analyses in eight healthy controls (black) and seven COVID patients (red).

included in the study (mean age 62 years, range 37-81). Three of them died, 11 were discharged after a few days (see Supporting information Table S1). Patients were compared to 11 healthy subjects (medical doctors or sanitary personnel) matched for gender, with a mean age of 43 years (range 27-61).

We recorded demographic data, medical history, symptoms, signs, temperature, and main laboratory findings from each patient. The total number and type of leukocytes in peripheral blood were analyzed by hemocytometer, according to routine methods. The main clinical and hematological data of these patients are reported in the Supporting information Tables S1-5. Some of them (i.e. patients 1, 2, 3, 9, 12, 13, 15-17) have already been described in a previous analysis of T-cell compartment and cytokine storm in subjects with COVID-19 pneumonia [14].

Blood collection and PBMC isolation

Twenty milliliters of blood was collected in vacuette containing EDTA and immediately processed according to biosafety rules [25]. Isolation of PBMC was performed by using Ficoll–Paque

according to standard procedures [15]. PBMC were stored in liquid nitrogen in FBS added with 10% DMSO until analysis. Plasma was then collected, centrifuged twice, and stored at −80°C until use.

In 11 patients, we could measure by standard methods the total amount of IgM, IgG, and IgA, along with the presence of IgM and IgG antibodies against rubella, *herpes simplex* type 1 and 2, *varicella-zoster*, measles, parotitis, influenza A and B, *Bordetella pertussis*, and, in the case of tetanus toxoid, IgG only. Finally, we measured anti-SARS-CoV2 antibodies, by using Vircell COVID-19 ELISA IgM$^+$ IgA and COVID-19 ELISA IgG, as indicated by the manufacturer (https://en.vircell.com/products/COVID-19-elisa/). Values are expressed as antibody index= (sample OD/cut-off serum mean OD) × 10.

B-cell immunophenotype by polychromatic flow cytometry

Thawed PBMC were stained with viability marker Promokine IR-840 (PromoCell GmbH, Heidelberg, Germany) for 20 min at room
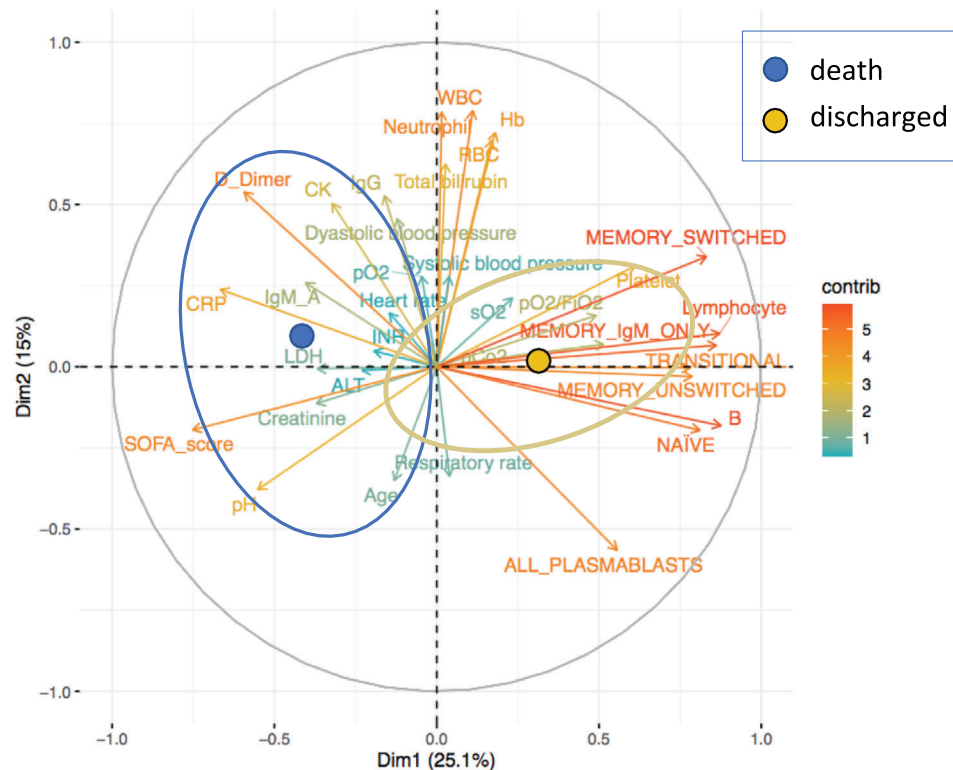
Figure 4. PCA shows that critical biomarkers and B cells are associated with clinical outcome. Absolute number of lymphocytes, platelets, total number of B lymphocytes, different types of B cells, pO_2/FiO_2, and sO_2 were associated with patients who were discharged (N = 11). On the contrary, IgM level, SOFA score, heart rate, blood pH, CK, CRP, D-dimer, among other clinical parameters, are localized in the area occupied by patients who died (N = 3). The areas circumscribed by the ellipses, where the colred dot indicates the center of the ellipse, represent the PCA space of the clinical events. Length and direction of the arrows indicate the weight and correlation that each parameter has in moving the center of the ellipse. The first two principal components accounted for >40% of the total data variance, and can locate in separate 2-D areas patients who died during the hospitalization from those who were discharged. Variables that lies in a given area of the plot are negatively correlated to those that lie on the opposite part of the plot.

temperature in PBS. One million PBMC were washed with FACS buffer and stained with DuraClone IM B cells containing the following lyophilized directly conjugated mAbs: IgD-FITC, CD21-PE, CD19-ECD, CD27-PC7, CD24-APC, CD38-AF750, IgM-PB, CD45-KrO. Cells were washed with FACS buffer and acquired at Cytoflex LX flow cytometer (Beckman Coulter, Hialeah, FL). A minimum of 500 000 cells was acquired on a CytoFLEX LX flow cytometer (Beckman Coulter) according to the state of the art methodology [25,26]. All reagents used in this study are reported in Supporting information Table S6.

Representation of high parameter flow cytometry

Flow Cytometry Standard (FCS) 3.0 files were imported into FlowJo software version 9 (Becton Dickinson, San Josè, CA), and analyzed by standard gating to remove aggregates and dead cells, and identify CD19$^+$ B cells IgM$^+$ or IgM$^-$ and/or IgD$^+$ or IgD$^-$. Then, 5000 IgM$^+$ IgD$^+$, or IgM$^+$IgD$^-$ or IgM$^-$IgD$^+$, or IgM$^-$IgD$^-$ B cells per sample were exported for further analysis in R, by following a script that makes use of Bioconductor libraries and R statistical packages (CATALYST 1.10.1). The script is available at https://github.com/HelenaLC/CATALYST). The selection

of cofactor for data transformation was checked on Cytobank (Beckman Coulter). FlowSOM (Bioconductor) was used to perform the metaclustering ($K = 20$); then, data were represented by the dimensionality reduction method named UMAP.

In vitro stimulation and proliferation assays

For proliferation assays, thawed isolated PBMCs were labeled with the fluorescent dye carboxyfluorescein succinimidyl ester (CFSE, from ThermoFisher, Eugene, OR). CFSE was used at a concentration of 1 μg/mL according to standard procedures [27]. Cells were then stimulated for 6 days with anti-CD3 plus anti-CD28 mAbs (1 μg/mL, Miltenyi Biotech, Bergisch Gladbach, Germany) and IL-2 (10 ng/mL). Flow cytometric analyses for the identification of cycling B cells were performed by gating CD19+ B cells, as described below.

Statistical analysis

The high dimensional cytometric analysis was performed by using differential discovery in high-dimensional cytometry via

high-resolution clustering [28,29]. Quantitative variables were compared by Mann–Whitney. Data are represented as individual values, means, and standard errors of the mean. Statistical analyses were performed using Prism 6.0 (GraphPad Software Inc., La Jolla, USA).

We have then investigated the role of B cells along with several biochemical parameters and a crucial clinical outcome, that is, death or discharge. For this purpose, we used the principal component analysis (PCA), a dimension reduction method that retains the characteristics of a data set that contribute most to its variance, by keeping lower order principal components (PCs) and ignoring the others. PCA uses an orthogonal transformation to collapse the dataset containing correlated parameters to a smaller set of linearly uncorrelated variables known as PCs (or dimension, "dim"), such that each PC is a weighted combination of all the markers. We performed this type of analysis in order to test whether subject classification was possible on the basis of the B-cell profile and/or clinical data. Thus, PCA was carried out on the clinical events (death or discharge, the so called "scores"), and a dataset comprising 34 parameters (the "variables") that included SOFA score, lymphocyte/μL, B cells/μL, naive B cells/μL, age, blood pH, pCo_2 (mmHg), pO_2 (mmHg), sO_2 (%), pO_2/FiO_2 ratio, ALT (U/L), total bilirubin (mg/dL), CK (U/L), creatinine (mg/dL), D-Dimer (ng/mL), Hb (g/dL), white blood cells, WBC (N/μL), red blood cells, RBC ($10^6/\mu$L), INR (ratio), LDH (U/L), CRP (mg/dL), platelets (10^9/L), respiratory rate (breaths/minute), systolic blood pressure (mmHg), dyastolic blood pressure (mmHg), heart rate (beats/minute), plasma IgG or IgM level, and different percentage of B-cell populations (naive, memory switched, memory IgM-only, transitional, memory unswitched, total plasmablasts), neutrophils ($10^3/\mu$L).

Conflict of interest: The authors declare no commercial or financial conflict of interest.

References

1 **Huang, C., Wang, Y., Li, X., Ren, L., Zhao, J., Hu, Y., Zhang, L. et al.,** Clinical features of patients infected with 2019 novel coronavirus in Wuhan, China. *Lancet* 2020. **395**: 497–506.

2 **Richardson, S., Hirsch, J. S., Narasimhan, M., Crawford, J. M., McGinn, T., Davidson, K. W.,** the Northwell COVID-19 Research Consortium, **et al.,** Presenting characteristics, comorbidities, and outcomes among 5700 patients hospitalized with COVID-19 in the New York City Area. *J. Am. Med. Assoc.* 2020. **323**: 2052–2059.

3 **Guaraldi, G., Meschiari, M., Cozzi-Lepri, A., Milic, J., Tonelli, R., Menozzi, M., Franceschini, E. et al.,** Tocilizumab in patients with severe COVID-19: a retrospective cohort study. *Lancet Rheumatol.* 2020.

4 **Cossarizza, A., De Biasi, S., Guaraldi, G., Girardis, M., Mussini, C. and** Modena Covid-19 Working Group (MoCo19), SARS-CoV-2, the virus that causes COVID-19: cytometry and the new challenge for global health. *Cytometry A* 2020. **97**: 340–343.

5 **Hamming, I., Timens, W., Bulthuis, M.L., Lely, A.T., Navis, G. and van Goor, H.,** Tissue distribution of ACE2 protein, the functional receptor for SARS coronavirus. A first step in understanding SARS pathogenesis. *J. Pathol.* 2004. **203**. 631–637.

6 **Allen, P., Soilleux, E., Pfefferle, S., Steffen, I., Tsegaye, T. S., He, Y., Gnirss, K. et al.,** Evidence that TMPRSS2 activates the severe acute respiratory syndrome coronavirus spike protein for membrane fusion and reduces viral control by the humoral immune response. *J. Virol.* 2011. **85**, 4122–4134.

7 **Frieman, M., Heise, M. and Baric R.,** SARS coronavirus and innate immunity. *Virus Res.* 2008. **133**: 101–112.

8 **Chen, I.-Y., Moriyama, M., Chang, M.-F. and Ichinohe T.,** Severe acute respiratory syndrome coronavirus viroporin 3a activates the NLRP3 inflammasome. *Front. Microbiol.* 2019. **10**: 50.

9 **Iwasaki A and Medzhitov R.,** Control of adaptive immunity by the innate immune system. *Nature Immunol.* 2015. **16**: 343–353.

10 **Huang, K. J., Su, I. J., Theron, M., Wu, Y. C., Lai, S. K., Liu, C. C. and Lei, H. Y.,** An interferon-gamma-related cytokine storm in SARS patients. *J. Med. Virol.* 2005. **75**: 185–194.

11 **Nie, Y., Wang, G., Shi, X., Zhang, H., Qiu, Y., He, Z., Wang, W. et al.,** Neutralizing antibodies in patients with severe acute respiratory syndrome–associated coronavirus infection. *J. Infect. Dis.* 2004. **190**: 1119–1126.

12 **Pan, Y., Zhang, D., Yang, P., Poon, L.L.M. and Wang, Q.,** Viral load of SARS-CoV-2 in clinical samples. *Lancet Infect. Dis.* 2020. **20**: 411–412.

13 **Cossarizza, A., Chang, H.D., Radbruch, A., Acs, A., Adam, D., Adam-Klages, S., Agace, W.W. et al.,** Guidelines for the use of flow cytometry

and cell sorting in immunological studies (second edition). *Eur. J. Immunol.* 2019. **49**: 1457–1973.

14 **De Biasi, S.**, **Meschiari, M.**, **Gibellini, L.**, **Bellinazzi, C.**, **Borella, R.**, **Fidanza, L.**, **Lo Tartaro, D.**, **Mattioli, M. et al.**, Marked T cell activation, senescence, exhaustion and skewing 2 towards TH17 in patients with Covid-19 pneumonia. *Nature Commun.* 2020. **11**: 3434.

15 **Lin, Y.**, **Kim, J.**, **Metter, E. J.**, **Nguyen, H.**, **Truong, T.**, **Lustig, A.**, **Ferrucci, L. and Weng, N. P.**, Changes in blood lymphocyte numbers with age in vivo and their association with the levels of cytokines/cytokine receptors. *Immunol. Ageing* 2016. **13**: 24.

16 **Blanco, E.**, **Pérez-Andrés, M.**, **Arriba-Méndez, S.**, **Contreras-Sanfeliciano, T.**, **Criado, I.**, **Pelak, O.**, **Serra-Caetano, A. et al.**, Age-associated distribution of normal B-cell and plasma cell subsets in peripheral blood. *J. Allergy Clin. Immunol.* 2018. **141**: 2208–2219.

17 **Dijkman, R.**, **Jebbink, M. F.**, **Deijs, M.**, **Milewska, A.**, **Pyrc, K.**, **Buelow, E.**, **van der Bijl, A. and van der Hoek, L.**, Replication-dependent downregulation of cellular angiotensin-converting enzyme 2 protein expression by human coronavirus NL63. *J. Gen. Virol.* 2012. **93**: 1924–1929.

18 **Rieckmann, P.**, **D'Alessandro, F.**, **Nordan, R. P.**, **Fauci, A. S. and Kehrl, J. H.**, IL-6 and tumor necrosis factor-alpha. Autocrine and paracrine cytokines involved in B cell function. *J. Immunol.* 1991. **146**: 3462–3468.

19 **Friederichs, K.**, **Schmitz, J.**, **Weissenbach, M.**, **Heinrich, P. C. and Schaper, F.**, Interleukin-6-induced proliferation of pre-B cells mediated by receptor complexes lacking the SHP/SOCS3 recruitment sites revisited. *Eur. J. Biochem.* 2001. **268**: 6401–6407.

20 **Jego, G.**, **Bataille, R. and Pellat-Deceunynck, C.**, Interleukin-6 is a growth factor for nonmalignant human plasmablasts. *Blood* 2001. **97**: 1817–1822.

21 **Chavele, K.-M.**, **Merry, E. and Ehrenstein, M. R.**, Cutting edge: circulating plasmablasts induce the differentiation of human T follicular helper cells via IL-6 production. *J. Immunol.* 2015. **194**: 2482–2485.

22 **Merluzzi, S.**, **Frossi, B.**, **Gri, G.**, **Parusso, S.**, **Tripodo, C. and Pucillo, C.**, Mast cells enhance proliferation of B lymphocytes and drive their differentiation toward IgA-secreting plasma cells. *Blood* 2010. **115**: 2810–2817.

23 **Frasca, D.**, **Romero, M.**, **Diaz, A.**, **Alter-Wolf, S.**, **Ratliff, M.**, **Landin, A. M.**, **Riley, R. L. and Blomberg, B. B.**, A molecular mechanism for TNF-α–mediated downregulation of B cell responses. *J. Immunol.* 2012. **188**: 279–286.

24 **Frasca, D.**, **Diaz, A.**, **Romero, M.**, **Landin, A. M. and Blomberg, B. B.**, High TNF-α levels in resting B cells negatively correlate with their response. *Exp. Gerontol.* 2014. **54**: 116–122.

25 **Cossarizza, A.**, **Gibellini, L.**, **De Biasi, S.**, **Lo Tartaro, D.**, **Mattioli, M.**, **Paolini, A.**, **Fidanza, L. et al.**, Handling and processing of blood specimens from patients with COVID-19 for safe studies on cell phenotype and cytokine storm. *Cytometry A* 2020. **97**.

26 **Nasi, M.**, **Pecorini, S.**, **De Biasi, S.**, **Bianchini, E.**, **Digaetano, M.**, **Neroni, A.**, **Lo Tartaro, D. et al.**, Altered expression of PYCARD, interleukin 1β, interleukin 18, and NAIP in successfully treated HIV-positive patients with a low ratio of CD4+ to CD8+ T cells. *J. Infect Dis.* 2019. **219**: 1743–1748.

27 **Quah, B. J. C. and Parish, C. R.**, The use of carboxyfluorescein diacetate succinimidyl ester (CFSE) to monitor lymphocyte proliferation. *J. Vis. Exp.* 2010. **44**: 2259.

28 **Weber, L. M.**, **Nowicka, M.**, **Soneson, C. and Robinson, M. D.**, diffcyt: differential discovery in high-dimensional cytometry via high-resolution clustering. *Commun. Biol.* 2019. **2**: 183.

29 **Roederer, M.**, **Nozzi, J. L. and Nason, M. C.**, SPICE: Exploration and analysis of post-cytometric complex multivariate datasets. *Cytometry A* 2011. **79**: 167–174.

Full correspondence: Andrea Cossarizza, Department of Medical and Surgical Sciences for Children and Adults, via Campi 287, 41125 Modena, Italy
e-mail: andrea.cossarizza@unimore.it